OFFICE OF NAVAL RESEARCH

Contract N00014-82-0280

Task No. NR413EOOI

TECHNICAL REPORT NO. 57

The Adsorption and Surface Reaction of $SiCl_4$ on Si(100)-(2x1)

by

Q. Gao, Z. Dohnalek, C.C. Cheng, W.J. Choyke and J.T. Yates, Jr.

Submitted To

Surface Science

Surface Science Center
Department of Chemistry
University of Pittsburgh
Pittsburgh, PA 15260

May 26, 1993

MASTER COPY - FOR REPRODUCTION PURPOSES

REPORT DOCUMENTATION PAGE

READ INSTRUCTIONS BEFORE COMPLETING FORM

1. REPORT NUMBER: 57	2. GOVT ACCESSION NO.
3. RECIPIENT'S CATALOG NUMBER	
4. TITLE (and Subtitle): The Adsorption and Surface Reaction of $SiCl_4$ on Si(100)-(2x1)	5. TYPE OF REPORT & PERIOD COVERED: Preprint
6. PERFORMING ORG. REPORT NUMBER	
7. AUTHOR(s): Q. Gao, Z. Dohnalek, C.C. Cheng, W.J. Choyke, and J.T. Yates, Jr.	8. CONTRACT OR GRANT NUMBER(s)
9. PERFORMING ORGANIZATION NAME AND ADDRESS: Surface Science Center, Department of Chemistry, University of Pittsburgh, Pittsburgh, PA 15260	10. PROGRAM ELEMENT, PROJECT, TASK AREA & WORK UNIT NUMBERS
11. CONTROLLING OFFICE NAME AND ADDRESS	12. REPORT DATE: May 26, 1993
	13. NUMBER OF PAGES: 25
14. MONITORING AGENCY NAME & ADDRESS (If different from Controlling Office)	15. SECURITY CLASS. (of this report): Unclassified
	15a. DECLASSIFICATION/DOWNGRADING SCHEDULE
16. DISTRIBUTION STATEMENT (of this Report)	
17. DISTRIBUTION STATEMENT (of the abstract entered in Block 20, if different from Report)	
18. SUPPLEMENTARY NOTES	
19. KEY WORDS (Continue on reverse side if necessary and identify by block number): Silicon, Chlorine, $SiCl_4$, Etching, Thin Films	

The adsorption and surface reaction of $SiCl_4$ on Si(100)-(2x1) have been investigated in the temperature range of 100K-1000K. Adsorption of monolayer $SiCl_4$ and multilayer $SiCl_4$ are observed by temperature programmed desorption (TPD), high resolution electron energy loss spectroscopy (HREELS), and electron stimulated desorption ion angular distribution (ESDIAD). Upon heating to ~ 200K and above, Si-Cl bond scission in adsorbed $SiCl_4$ occurs, depositing $SiCl_x$ species. Heating to 673K leaves the surface with only silicon monochloride species, SiCl(a), exhibiting Si-Cl stretching mode, $\nu SiCl$, at ~ 560 cm^{-1}, and a Cl^+ ESDIAD pattern indicative of inclined Si-Cl bond directions from Cl adsorbed on Si_2 dimer sites. Silicon substrate etching occurs above 800K producing $SiCl_2(g)$ as the desorption product.

Submitted to: Surface Science

Date: 5/26/93

The Adsorption and Surface Reaction of $SiCl_4$ on Si(100)-(2x1)

Q. Gao. Z. Dohnalek, C C. Cheng, W. J. Choyke* and J. T. Yates, Jr.

Surface Science Center
Department of Chemistry
University of Pittsburgh
Pittsburgh, PA 15260

*Department of Physics
University of Pittsburgh
Pittsburgh, PA 15260

The Adsorption and Surface Reaction of $SiCl_4$ on Si(100)-(2x1)

Q. Gao. Z. Dohnalek, C. C. Cheng, W. J. Choyke* and J. T. Yates, Jr.

Surface Science Center, Department of Chemistry,
University of Pittsburgh, Pittsburgh, PA 15260

*Department of Physics, University of Pittsburgh, Pittsburgh, PA 15260

Abstract

The adsorption and surface reaction of $SiCl_4$ on Si(100)-(2x1) have been investigated in the temperature range of 100K-1000K. Adsorption of monolayer $SiCl_4$ and multilayer $SiCl_4$ are observed by temperature programmed desorption (TPD), high resolution electron energy loss spectroscopy (HREELS), and electron stimulated desorption ion angular distribution (ESDIAD). Upon heating to ~ 200K and above, Si-Cl bond scission in adsorbed $SiCl_4$ occurs, depositing $SiCl_x$ species. Heating to 673K leaves the surface with only silicon monochloride species, SiCl(a), exhibiting Si-Cl stretching mode, νSiCl, at ~ 560 cm^{-1}, and a Cl^+ ESDIAD pattern indicative of inclined Si-Cl bond directions from Cl adsorbed on Si_2 dimer sites. Silicon substrate etching occurs above 800K producing $SiCl_2$(g) as the desorption product.

1. Introduction

Silicon chloride and chlorosilane molecules ($SiCl_4$, Si_2Cl_6,and SiH_2Cl_2, etc.) play an important role in the chemical vapor deposition (CVD) as well as in the dry etching of Si substrates. Silicon chloride and chlorosilane molecules have

been widely used as the source material for the growth of thin films of silicon, silicon nitride, silicon carbide and silicon dioxide [1-7]. These molecules are also the common reaction products in ion [8-9] or photon assisted silicon etching [10-11] processes. Therefore, it is important to understand the chemisorption and surface reaction of these molecules for better control of the CVD and the etching processes, since they are the transport species between the gas phase and the surface in both thin film growth and in etching.

There are a few previous studies of silicon chloride surface chemistry which are limited to the Si(111)-(7x7) substrate. The chemisorption and thermal decomposition of silicon chloride, $SiCl_4$, on Si(111)-(7x7) have been investigated with laser induced thermal desorption (LITD) and temperature programmed desorption (TPD) techniques [12]. It is observed that the reactive sticking coefficient for $SiCl_4$ is small ($S_0 \sim 0.18$ at 160K) and that this coefficient decreases with increasing substrate temperature ($S_0 \sim 0.03$ at 600K). This is interpreted with a precursor-mediated adsorption model where the first stage of adsorption involves trapping of $SiCl_4$ in a weakly-bound precursor state. Compared to the SiH_4 surface chemistry, where H_2 is the primary desorption product [13], thermal decomposition of $SiCl_4$ on Si(111)-(7x7) gives $SiCl_2$ as the primary desorption product (as opposed to Cl_2) with second-order desorption kinetics ($E_d = 65 \pm 5$ kcal/mole, $\nu_d = 3.2 \pm 0.7$ cm^2/s) [12]. Soft x-ray photoemission spectroscopy (SXPS) combined with thermal desorption studies indicate that upon adsorption at room temperature, $SiCl_4$ completely dissociates on Si(111)-(7x7) yielding only surface monochloride species, SiCl(a). In contrast, Si_2Cl_6 partially dissociates into $SiCl_x$ (x=1, 2, 3) fragments upon adsorption at room temperature [14]. Dichlorosilane (SiH_2Cl_2) adsorption on Si(111) is also

found to adsorb by a precursor-mediated process yielding H_2, HCl and $SiCl_2$ as the decomposition products [15].

The surface chemistry of silicon chloride on the more technologically relevant Si(100) substrate, however, has not been studied to our knowledge. On Si(100)-(2x1), core-level soft x-ray photoelectron spectroscopy (SXPS) studies indicate that at temperatures ranging from 298 - 1073K, dichlorosilane chemisorbs dissociatively forming silicon monochloride surface species [16]; higher silicon chloride species are not observed.

In this paper, we report studies of the adsorption and chemical bonding of $SiCl_4$ on the Si(100)-(2x1) substrate as well as the spectroscopic characterization of the surface reaction intermediates. The fundamental questions addressed are the $SiCl_4$ bonding states and bonding configurations, the surface species formed from $SiCl_4$ chemisorption at elevated temperatures, and the surface reaction products which desorb. To answer these questions, a combination of surface probes are employed including temperature programmed desorption (TPD), high resolution electron energy loss spectroscopy (HREELS), and electron stimulated desorption ion angular distribution (ESDIAD). The Si-Cl bond orientations are monitored by ESDIAD, a measurement technique with a precision of ~ 1° [17a-c]

2. Experimental

Experiments were carried out in two UHV chambers. The first chamber was equipped with a digital ESDIAD/LEED (electron stimulated desorption ion angular distribution/low energy electron diffraction) apparatus, an Auger electron spectrometer (AES), a quadrupole mass spectrometer (QMS) for line-of-sight temperature programmed desorption (TPD), and an additional QMS for ion mass

analysis in ESD. The second UHV chamber housed a high resolution electron energy loss spectrometer (HREELS), LEED, AES and a QMS for TPD. The primary beam energy used for the HREELS study was 4.2 eV and the full width at half maximum (FWHM) of the elastic beam was about 65 cm^{-1}. Flux-calibrated micro capillary-collimated gas dosers [18,19] were used in both chambers for control of the $SiCl_4$ exposure. $SiCl_4$ was purchased from Aldrich company with a purity of 99.999%. Before use, it was further purified by several freeze-pump-thaw cycles in the gas line. The Si(100) single crystal was cleaned by Ar^+ sputtering and subsequent annealing at 1173K. The crystal temperature was measured by a chromel-constantan thermocouple enclosed in a Ta-foil envelope which was inserted into a slot on the crystal edge [18]. The base pressure in both UHV chambers was $1x10^{-10}$ mbar or below.

3. Results

3.1 Temperature Programmed Desorption Studies

To characterize the adsorption kinetics and the binding states of $SiCl_4$ on Si(100)-(2x1), temperature programmed desorption was employed as shown in fig. 1. Here, we employ line-of-sight geometry through a small aperture (diameter is 5 mm) for detecting the desorption from the Si(100)-(2x1) surface. Following the adsorption of $SiCl_4$ on Si(100)-(2x1) at 125K, the detected desorption products include three $SiCl_4$ desorption features (monitored by the parent ion $SiCl_4^+$, m/e=168 amu) at 132K, 142K and 230K, respectively, and a single $SiCl_2$(g) desorption feature (monitored with $SiCl^+$ m/e=63 amu, the major cracking product of $SiCl_2$(g) in the ionizer) with a peak temperature at ~860K. No Cl_2(g) desorption was observed as was reported for $SiCl_4$/Si(111) [14]. The desorption feature at ~132K does not saturate for higher $SiCl_4$ exposures and is thus

attributed to multilayer $SiCl_4$ adsorption. $SiCl_4$ desorption at 230K is observed only above $SiCl_4$ exposures of $0.7x10^{14}/cm^2$, below which either there is no population of this adsorption state or the desorption signal is buried in the noise preventing measurement.

The adsorption kinetics for the first adsorbed $SiCl_4$ layer (142K peak) is shown in the insert of fig.1. At an exposure of ~$1.7x10^{14}$ $SiCl_4/cm^2$, a monolayer is completed. We observe, however, that the multilayer desorption feature has appeared (at an exposure of ~$1.2x10^{14}$ $SiCl_4/cm^2$) before the full monolayer is completed.

The $SiCl_2(g)$ desorption is shown from $SiCl_4$ decomposition with a peak temperature of ~860K at $1.7x10^{14}$ $SiCl_4/cm^2$ initial exposure. The peak temperature is shifted to lower temperatures for increasing exposure. The $SiCl_2(g)$ desorption feature has been observed for all the $SiCl_4$ exposures studied here. The amount of Si desorbed in $SiCl_2(g)$ at $1.7x10^{14}$ $SiCl_4/cm^2$ exposure is estimated of about 0.04 of a monolayer.

3.2 Low Temperature Adsorption of $SiCl_4$/Si(100)-(2x1) - HREELS Studies

As shown in fig. 2, adsorption of $SiCl_4$ at 100K produces a vibrational spectrum similar to that of gas phase $SiCl_4$ molecules. At a $SiCl_4$ exposure of $0.67x10^{14}$ molecules/cm^2, a strong loss peak is observed at 630 cm^{-1} together with a medium intensity peak at 220 cm^{-1} (fig. 2a). These two peaks are assigned to the degenerate asymmetric SiCl stretching mode, $\nu_d SiCl_4$ (ν_3), and the degenerate umbrella bending mode of the $SiCl_3$ moiety, δ_d (ν_4), of the $SiCl_4$(a) molecules, respectively [20]. Extremely weak peaks at 390 cm^{-1}, 850 cm^{-1}, 1260

cm^{-1} and 2080 cm^{-1} are seen as well. It appears that the local point group symmetry of the $SiCl_4$ molecules is close to T_d which would give only two dipole active modes: a degenerate Si-Cl stretching mode, $\nu_d SiCl_4$ (ν_3), and the umbrella bending mode, $\delta_d(\nu_4)$, of the $SiCl_3$ moiety. The symmetric stretching mode, ν_s $SiCl_4$ (ν_1), at ~ 400 cm^{-1} and the scissors mode, δ_d (ν_2), at ~145 cm^{-1} [20] are forbidden by the dipole selection rule due to the local T_d symmetry. These modes, however, may be excited by the impact scattering mechanism. A weak loss for the symmetric stretching mode at ~390 cm^{-1} is barely observed and the scissors mode of $SiCl_4$ (~150 cm^{-1}) is not observed in this study. At an exposure of 1.7×10^{14} $SiCl_4/cm^2$, nearly the same vibrational features are observed (fig. 2b). The previous 630 cm^{-1} peak shifts slightly upward to 635 cm^{-1}. At an exposure of 3.4×10^{14} $SiCl_4/cm^2$, the HREEL spectrum displays an enhancement of the 860 cm^{-1} and the 1280 cm^{-1} peaks (fig. 2c). The 860 cm^{-1} peak may be a combination band of the 220 cm^{-1} and 640 cm^{-1} modes. Double loss scattering (with energy losses of 220 cm^{-1} and 640 cm^{-1}) can also contribute to this peak. The 1280 cm^{-1} peak is assigned to the overtone of the 640 cm^{-1} peak. Like the 860 cm^{-1} peak, a double loss (with energy losses of 640 cm^{-1} and 640 cm^{-1}) scattering may also contribute. The small probabilities for the double losses and the overtone processes are consistent with the weak intensities of these peaks. For small surface coverages, the bare silicon surface sites are easily attacked by the background water producing a surface hydroxyl group and silicon monohydride. The former has a vibrational feature at 800-900 cm^{-1} and the latter has the Si-H stretching mode at ~2080 cm^{-1} [21], and weak features in these regions are also observed.

3.3 Temperature Dependent Behavior of $SiCl_4$/Si(100)-(2x1)

A multilayer initial exposure at 100K results in a HREEL spectrum shown in fig. 3a. The spectrum is identical to fig. 2c. Annealing to 200K removes the multilayer and monolayer $SiCl_4$ and causes shifts of the 640 cm^{-1} peak to 577 cm^{-1}, the 220 cm^{-1} peak to 210 cm^{-1}, and the 390 cm^{-1} peak to 400 cm^{-1} (fig. 3b). The increase in relative intensity ratios of the 400 cm^{-1} peak to both the 210 cm^{-1} peak and the 577 cm^{-1} peak is observed (fig. 3b) compared to the ratios of the 390 cm^{-1} peak to both the 220 cm^{-1} peak and the 640 cm^{-1} peak (fig.3a). This is an indication of the breakdown of the local T_d symmetry of the $SiCl_4$ species, probably by partial decomposition. A weak loss peak at 900 cm^{-1} is associated with the vacant sites generated by $SiCl_4$ desorption at 200K and is thus likely to be from the background water adsorption. After 300K annealing, the Si-Cl stretching mode shifts down further to 566 cm^{-1} (fig 3c). The 400 cm^{-1} feature is still observable. Further annealing to 673K leads to the disappearance of both the 200 cm^{-1} peak and the peak at ~800 cm^{-1} (fig. 3d), consistent with the final formation of a surface monochloride species, as previously observed for Cl_2 and HCl adsorption on Si(100) [22-23]. The formation of surface monochloride species also leads to the peak intensity enhancement of the Si-Cl stretching mode at 566 cm^{-1} as observed in fig. 3d. A reduction in the peak intensity and a shift of the 566 cm^{-1} peak to 560 cm^{-1} are observed after annealing to 847K (fig. 3e) which is correlated with the depletion of surface chlorine by the thermal desorption of $SiCl_2$(g) (fig. 1).

3.4 ESDIAD Studies of $SiCl_4$/Si(100)-(2x1)

In the ESDIAD experiment, the surface species containing Cl are subjected to electron beam excitation. The transition of the Si-Cl bond from the ground electronic state to an excited anti-bonding electronic state leads to Cl desorption and ionization (Cl^+). The trajectories of the Cl^+ ions are recorded and summed together in ESDIAD which indicate the distribution of the spatial orientation of the Si-Cl chemical bonds. Adsorption of $SiCl_4$ at 120K to multilayer coverage results in a Cl^+ ESDIAD pattern shown in fig. 4a. The pattern consists of a strong central beam and a nearly uniform azimuthal intensity distribution. Annealing to 200K results in four shoulder peaks in the <011> and <01$\bar{1}$> azimuth, superimposed on a central beam (fig. 4b). Annealing to 300K causes an enhancement of the normal Cl^+ beam (fig. 4c). An ESDIAD pattern primarily exhibiting four off-normal Cl^+ beams is observed after annealing the surface to 673K (fig. 4d). These four beams correspond to the orientations of the Si-Cl bonds on the Si_2 dimers in the two orthogonal domains. Similar ESDIAD patterns have been observed for chlorine adsorption on Si(100)-(2x1) at the same annealing temperature [22, 24] and for the HCl adsorption on Si(100)-(2x1) at 120K [23]. Surface monochloride species are responsible for these four off-normal emission beams for the three adsorption systems at this annealing temperature. A decrease of the beam intensities is observed after 847K annealing (fig. 4e). Heating to this temperature leads to the etching of the substrate with $SiCl_2$(g), causing a decrease of the Cl^+ ion intensity. The approach to a more random orientation of the Si-Cl bonds for the remaining SiCl(a) species on an etched substrate is indicated by the merging of the four shoulder beams with the broad central beam; similar ESDIAD pattern changes are observed for Cl_2 adsorption onto Si(100) followed by heating to 847K [22].

4. Discussion

4.1 The Bonding of $SiCl_4$ on Si(100)-(2x1) at Low Temperatures

Three $SiCl_4$ desorption states are detected (fig. 1) in the TPD experiments. In order of increasing desorption temperature, they are the multilayer $SiCl_4$(a) (T_p~132K), physisorbed $SiCl_4$ within the monolayer range (T_p~142K), and a small amount of $SiCl_4$ (≤ 0.01 of the first layer $SiCl_4$(a)) with a peak temperature at ~ 230K. The monolayer $SiCl_4$ reaches saturation coverage with increasing exposure (Fig. 1 insert) while the multilayer does not show saturation behavior. Both monolayer and multilayer $SiCl_4$(a) display vibrational spectra similar to that of the gas phase molecules, indicative of non-dissociative adsorption (see fig. 2 and the summary of the vibrational mode assignments in Table 1). The lack of a scissors mode peak (~145 cm^{-1}) and the extremely weak peak, if any, for the symmetric Si-Cl stretching mode (~390 cm^{-1}) (fig.2a) suggest that the local symmetry of the $SiCl_4$ molecules is nearly the same as for the free $SiCl_4$ molecule (T_d). Since the physisorbed monolayer and multilayer molecules are bound to the surface by means of van der Waals forces as opposed to strong directional covalent chemical bonding, a random Si-Cl bond orientation is, therefore, expected. This is confirmed by the nearly uniform azimuthal Cl^+ ion intensity distribution in ESDIAD measurements shown in the contour plot (fig.4a). The angular distribution shows a maximum in the surface normal direction (with polar angle $\Theta = 0$) due to the lowest neutralization probability for Cl^+ ions departing in this direction. According to Hagstrum [25], the rate of Cl^+ ion neutralization is exponentially related to the ion-surface separation (z):

$$R = A \exp(-a z)$$

where $z \propto d \cdot \cos\Theta$, d is the Si-Cl bond length and Θ is the polar angle of the Si-Cl bond relative to the surface normal. This leads to a minimized neutralization probability for Cl^+ ions leaving in the direction of surface normal (Θ=0).

Small amounts (≤ 0.01 of the first layer) of $SiCl_4$ desorption (Tp~230K) are clearly observed for $SiCl_4$ exposures above 0.7×10^{14} $SiCl_4/cm^2$. The following arguments favor recombinative desorption of $SiCl_x(a) + (4-x)Cl(a) \rightarrow SiCl_4(g)$ as the origin of the 230K $SiCl_4$ desorption state: (1) HREEL spectra show the symmetric Si-Cl stretching mode at ~ 400 cm^{-1} with moderate intensity, indicative of a breakdown of the local T_d symmetry for the $SiCl_x$ species remaining after desorption of $SiCl_4$ at 200K (fig. 3b). This can be interpreted as being due to the dissociation of $SiCl_4(a)$ into $SiCl_3(a)$; (2) The vibrational features are close to those found for CH_3SiCl_3 molecules. The asymmetric SiCl stretching mode, ν_a at 576 ~ 578 cm^{-1}, symmetric SiCl stretching, ν_s at 450 ~ 458 cm^{-1}, and the bending and rocking modes, δ and γ, in the range of 164 ~ 229 cm^{-1}, for this molecule have been observed [26a-c]. These modes correspond well with the HREELS peaks observed at 577 cm^{-1}, 400 cm^{-1} and 210 cm^{-1} in fig. 3b; (3) In ESDIAD, annealing to 200K causes the development of the four shoulder peaks along the <011> and <01$\bar{1}$> directions. These shoulders in the ion angular distribution of Cl^+ are due to the contribution from the surface monochloride species produced from $SiCl_4$ decomposition with Cl captured on the Si(100) substrate [22-24]. An unlikely alternative explanation for the species responsible for the 230K $SiCl_4$ desorption process is the production of a distorted $SiCl_4$ species of low coverage on the surface (such as on defect sites).

4.2 The Surface Decomposition of $SiCl_4$ on Si(100)-(2x1)

Beyond a temperature of ~250K, $SiCl_4$ ceases to be a thermal desorption product from the Si(100)-(2x1) surface. Both HREELS and AES measurements show that chlorine remains behind above 250K indicating that $SiCl_4$(a) has decomposed to lower silicon chloride species which are strongly bound. As shown in fig. 3, the ~ 200 cm^{-1} δ bending mode for $SiCl_x$ (a) species remains up to 300K, as does the 400 cm^{-1} symmetric stretching mode for $SiCl_x$(a). It is not possible to discriminate between modes due to $SiCl_3$(a) and $SiCl_2$(a) on the basis of these observed frequencies [26a-d]. At 673K in fig. 3, the vibrational spectrum is closely similar to that found for Cl_2 adsorption on Si(100)-(2x1) at the same temperature; the 566 cm^{-1} mode corresponds to the asymmetric stretching mode, ν_aSiCl, at low chlorine coverages. The vibrational frequencies of different silicon chlorides observed in this study and those reported in the literature are summarized in Table 1.

ESDIAD results also indicate that inclined Si-Cl bonds are forming as $SiCl_4$-derived surface species decompose. Fig. 4d, obtained after heating to 673K, is closely similar to the Cl^+ ESDIAD pattern produced from Cl_2 adsorption on Si(100) at 100K followed by 673K annealing [22,24]. This pattern is dominated by four Cl^+ beams lying in the vertical planes parallel to the Si_2 dimer bonds in two orthogonal domains on the crystal, and this pattern and the measured Si-Cl bond angle (25°±4°) have been extensively discussed previously [22]. Annealing to 847K (fig. 4e) results in a diminished contribution of the four Cl^+ beams, coupled to a broad normally oriented Cl^+ beam as is also observed for Cl_2-derived layers (annealed at 847K) on Si(100)-(2x1). This is due to surface etching with liberation of $SiCl_2$(g), producing randomized Si-Cl bond orientations [22].

$SiCl_2$ desorption near 800K occurs from a surface containing only SiCl(a) species. Thus $SiCl_2(g)$ must be formed from a recombination process. Assuming second-order kinetics in surface chlorine coverage, we derive an activation energy of 83±7 kcal/mole using the method of Chan et al. [27]. Laser induced thermal desorption studies of $SiCl_2$ from $SiCl_4$/Si(111)-(7x7) yield an activation energy of 65±5 kcal/mole for second-order desorption kinetics [12].

A summary of the thermal processes observed in this work, and the temperature employed to observe these processes is given below:

$$SiCl_4(a)(\text{multilayer}) \xrightarrow{132K} SiCl_4(g)$$

$$SiCl_4(a)(\text{monolayer}) \xrightarrow{142K} SiCl_4(g)$$

$$SiCl_4(a)(\text{monolayer}) \xrightarrow{\geq 200K} SiCl_x(a) + (4-x)\ SiCl(a)$$

$$SiCl_x(a) + (4-x)\ SiCl \xrightarrow{230K} SiCl_4(g)$$

$$SiCl_x(a)\ (x=2, 3) \xrightarrow{673K} x\ SiCl(a)$$

$$SiCl(a) + SiCl(a) \text{ or } Cl(a) \xrightarrow{\geq 800K} SiCl_2(g)$$

4.3 The Surface Structure Controlled Chemistry

A fundamental question in surface science concerns the role of the detailed surface structure in determining surface chemical processes. It appears that the detailed surface structure does play a role for the $SiCl_4$ surface dissociation process. With soft x-ray photoemission spectroscopy (SXPS) and thermal desorption studies it is observed that upon adsorption at room temperature, $SiCl_4$ completely dissociates on Si(111)-(7x7) yielding *only surface monochloride*

species SiCl(a) [14]. However, from the studies presented here the low temperature adsorption of $SiCl_4$ on Si(100)-(2x1) followed by annealing to 300K does not completely dissociate $SiCl_4$(a). Therefore, in comparison with the Si(111)-(7x7) surface, the Si(100)-(2x1) surface is less reactive for $SiCl_4$ dissociation.

It is well understood that on the Si(111)-(7x7) surface, large backbond strain is present for the adatoms compared to the rest atoms [28-29]. The strained Si-Si backbonds are, from a thermodynamic point of view, active in chemical reactions. This may explain why $SiCl_4$(a) molecules can dissociate completely into surface monochloride species at room temperature on Si(111)-(7x7). On the other hand, only partial dissociation of $SiCl_4$ occurs on the Si(100)-(2x1) surface at 300K, indicative of less bond strain for the Si(100)-(2x1) surface [30]. A similar bond strain effect has been observed for the dissociation of NH_3 molecules [31] where on Si(111)-(7x7), NH_3 is dissociated into NH(a) at 300-600K while on Si(100)-(2x1), the NH_2(a) species is stable up to 600K. In addition, STM studies of hydrogen on Si(111)-(7x7) provide convincing experimental evidence that the strained adatom backbond exhibits a lower reaction barrier toward atomic hydrogen than the unstrained rest atom backbond [32].

4.4 Correlation with Chemical Vapor Deposition of Silicon Films from $SiCl_4$

In the high temperature chemical vapor deposition (CVD) of silicon thin films, mixtures of H_2 and $SiCl_4$ gas are admitted to the growth chamber in the temperature range of 1000K-1300K [33-34]. Based on the results of our investigation in this paper, the most likely surface species to be present in this

temperature range is SiCl(a). In the low temperature CVD process, like catalytic CVD ($T_{substrate}$ <573K) [35], decomposition of $SiCl_4$ occurs on a hot filament delivering $SiCl_x$(x=1, 2, 3) species to the surface where also monochloride surface species would likely form. Hydrogenation to produce HCl leaves the silicon film. Current studies of these processes are limited to spectroscopic monitoring of gas phase products [36].

5. Conclusions

The following results are found for the adsorption and decomposition of $SiCl_4$ on Si(100)-(2x1).

1. Multilayer and monolayer adsorption of $SiCl_4$ has been observed. Multilayer desorption occurs at 132K; monolayer desorption occurs at 142K.
2. A small quantity ($\leq$ 0.01 of the first layer) of $SiCl_4$ desorbs at 230K and is postulated to be due to a recombination process between $SiCl_x$ species.
3. Heating in the temperature range 300-673K results in the loss of $SiCl_4$ species forming Si-Cl bonds which have similar vibrational and directional properties to the Si-Cl bonds formed on Si(100)-(2x1) from Cl_2 in the same surface temperature range.
4. Above ~800K, $SiCl_2$(g) species desorb with an activation energy of 83±7 kcal/mole assuming second-order kinetics in chlorine coverage.

Acknowledgment

We thank the Office of Naval Research for support of this work.

References

1. P. van der Putte, L. J. Giling and J. Bloem, J. Cryst. Growth 31 (1975)299.
2. S. Motojima, M. Iwamori and T. Hattori, J. Mater. Sci. 21 (1986) 3836.
3. R. C. Taylor, B. A. Scott, S. T. Lin, F. LeGouse and J. C. Tsang, MRS Symp. Proc. 77 (1987) 709.
4. R. C. Taylor and B. A. Scott, MRS Symp. Proc. 105 (1988) 319.
5. R. C. Taylor and B. A. Scott, J. Electrochem. Soc. 136 (1989) 2382.
6. C. W. Pearce, in VLSI Technology, 2nd ed., S. M. Sze ed. Chap. 2, McGraw-Hill, New York, 1988.
7. S. K. Ghandhi, VLSI Fabrication Principles, Chap. 5, Wiley, New York, 1983.
8. M. C. Chuang and J. E. Coburn, J. Vac. Sci. Technol. A8 (1990) 1969.
9. J. O. Chinn and J. E. Coburn, J. Vac. Sci. Technol. B3 (1985) 410.
10. R. B. Jackman, H. Ebert and J. S. Foord, Surf. Sci. 176 (1986) 183.
11. W. Sesselman and T. J. Chuang, J. Vac. Sci. Technol. B3 (1985) 1507.
12. P. Gupta, P. A. Coon, B. G. Koehler and S. M. George, J. Chem. Phys. 93(4) (1990) 2827.
13. R. Imbihl, J. E. Demuth, S. M. Gates and B. A. Scott, Phys. Rev. B39 (1989) 5222.
14. L. J. Whitman, S. A. Joyce, J. A. Yarmoff, F. R. McFeely and L. J. Terminello, Surf. Sci. 232 (1990) 297.
15. P. A. Coon, P. Gupta, M. L. Wise and S. M. George, J. Vac. Sci. Technol. A(10) (1992) 324.
16. J. A. Yarmoff, D. K. Shuh, T. D. Durbin and C. W. Lo, D. A. Lapiano-Smith, F. R. McFeely and F. J. Himpsel, J. Vac. Sci. Technol. A10 (1992)2303.
17. (a) R. D. Ramsier and J. T. Yates, Jr., Surf. Sci. Reports, 12 (1991) 243.

(b) J. T. Yates, Jr., M. D. Alvey, M. J. Dresser, M. A. Henderson, M. Kiskinova, R. D. Ramsier and A. Szabo, Science, 225 (1992) 1397.

(c) T. E. Madey, Science, 234 (1986) 316.

18. M. J. Bozack, L. Muehlhoff, J. N. Russell, Jr., W. J. Choyke, and J. T. Yates, Jr., J. Vac. Sci. Technol. A5, (1987),1.

19. A. Winkler and J. T. Yates, Jr., J. Vac. Sci. and Technol. A6 (5) (1988) 2929.

20. K. Nakamoto, in Infrared Spectra of Inorganic and Coordination Compounds, 4th ed, p. 132, New York, John Wiley and Sons, Inc., 1986, and references therein.

21. H. Ibach, H. Wagner and D. Bruchmann, Solid State Commun. 42 (1982) 457.

22. Q. Gao, C.C. Cheng, P. J. Chen, W. J. Choyke and J. T. Yates, Jr., J. Chem. Phys., in print, and references therein.

23. Q. Gao, C. C. Cheng, P. J. Chen, W. J. Choyke and J. T. Yates, Jr., Thin Solid Films, 225 (1993) 140, and references therein.

24. C.C. Cheng, Q. Gao, W. J. Choyke and J. T. Yates, Jr. Phys. Rev. B46 (1992) 12810.

25. H. D. Hagstrum, Phys. Rev. 123 (1961) 758.

26. (a) M. C. Tobin, J. Am. Chem. Soc. 75 (1953) 1788 and references therein.

(b) K. Shimizu and H. Murata, Bull. Chem. Soc. Japan 32 (1959) 46 and references therein.

(c) L. Burnelle and J. Duchesne, J. Chem. Phys. 20 (1952) 1324.

(d) J. Laane, Spectrochimica Acta, 26A (1970) 517.

27. C.-M. Chan, R. Aris and W. H. Weinberg, Appl. Surf. Sci. 1 (1978) 360.

28. I. K. Robinson, W. K. Waskiewicz, P. H. Fuoss and L. J. Norton, Phys. Rev. B 37 (1988) 4325.

29. R. D. Meade and D. Vanderbilt, Phys. Rev. B 40 (1989) 3905.

30. A general review is available in: The Chemical Physics of Solid Surfaces and Heterogeneous Catalysis, Vol. 5, Eds. D. A. King and D. P. Woodruff, Elsevier, Amsterdam, 1988, Chap. 2 by M. Schluter, p.37, and references therein.
31. P. J. Chen, M. L. Colaianni and J. T. Yates, Jr. Surf. Sci. Lett. 274 (1992) L605.
32. J. J. Boland, Surf. Sci. 244 (1991)1.
33. V. S. Ban, J. Electrochem. Soc. 122 (1975) 1389.
34. T. Aoyama, Y. Inoue, and T. Suzuki, J. Electrochem. Soc. 130 (1983) 203.
35. H. Matsumura and H. Ihara, J. Appl. Phys. 64 (1988) 6505.
36. J. Nishizawa and H. Sakuraba, Surf. Sci. Rep. 15 (1992) 137.

Figure Captions

Fig 1. Temperature programmed desorption of a multilayer $SiCl_4$(a) adsorbed on Si(100)-(2x1) at 125K. The exposure is $1.7x10^{14}$ $SiCl_4/cm^2$. The $SiCl_2$(g) desorption feature from $SiCl_4$ decomposition is displayed for T>800K. Lower temperature $SiCl^+$ signals correspond to the $SiCl_4$(g) cracking in the mass spectrometer. The insert indicates the development of the TPD yield for the monolayer of $SiCl_4$ versus exposure (142K peak).

Fig. 2. HREEL spectra of $SiCl_4$ adsorption on Si(100)-(2x1) at 100K with $SiCl_4$ exposures: (a) $0.67x10^{14}/cm^2$; (b) $1.7x10^{14}/cm^2$; (c) $3.4x10^{14}/cm^2$.

Fig. 3. Thermal development of HREEL spectra for $SiCl_4$/Si(100)-(2x1). The initial $SiCl_4$ exposure is $3.4x10^{14}/cm^2$. (a) 100K adsorption; then annealed

to the following temperatures: (b) 200K; (c) 300K; (d) 673K and (e) 847K. All spectral data are collected at 100K.

Fig.4. Thermal development of the Cl^+ ESDIAD pattern produced from $SiCl_4$ adsorption. Electron beam energy E_e = 120V, crystal current I_e = 2pA, $V_{bias\ (on\ crystal)}$ = +10V. (a) 120K adsorption of $3.4x10^{14}$ $SiCl_4/cm^2$. Then annealed to the following temperatures: (b) 200K; (c) 300K; (d) 673K; and (e) 847K. All data are collected at 120K.

Table 1. Vibrational Frequencies for Silicon Chlorides (cm^{-1})

	$\upsilon_d SiCl_4(\upsilon_3)$	$\upsilon_s SiCl_4(\upsilon_1)$	$\delta_d SiCl_3(\upsilon_4)$	$\delta_d SiCl_2(\upsilon_2)$
$SiCl_4$(g) [20]	616.5	423	220	145
$SiCl_4$(a) [this work]	630-640	390	220	

	$\upsilon_a SiCl$	$\upsilon_s SiCl$	$\delta SiCl$	$\gamma SiCl$
$SiCl_3(CH_3)$(g) [26a-c]	576-578	450-458	164-229	229
$SiCl_2(CH_3)_2$(g) [26a]	533	465	169	
$SiCl_2(CH_2)_3$(g) [26d]	533	376	167-241	
$SiCl_x$(a) (x=2,3) [this work]	566-577	400	200-210	

	$\upsilon SiCl$
$SiCl(CH_3)_3$(g) [26a]	467
SiCl(a) [23]	553-600
SiCl(a) [this work]	560-566

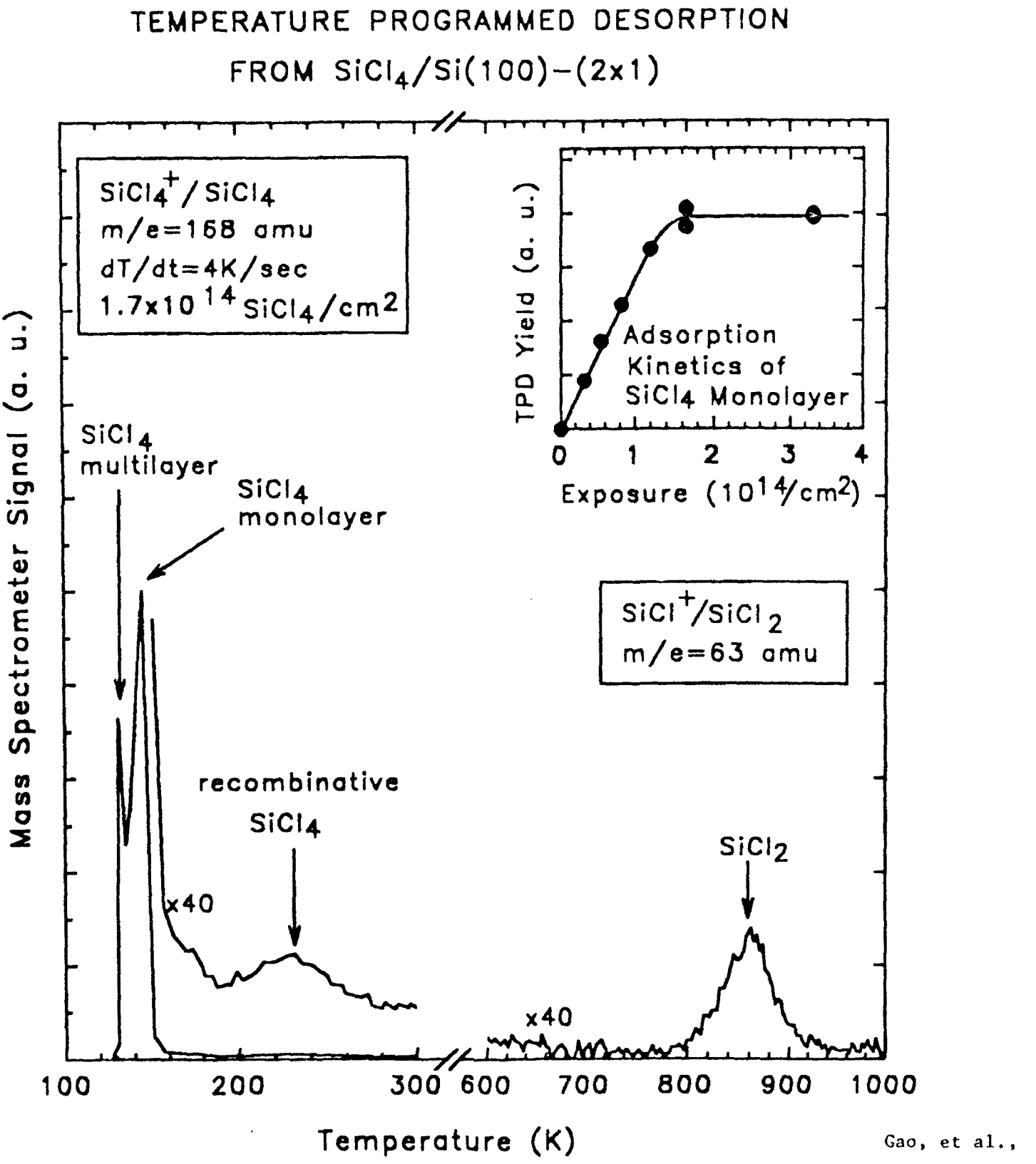

Gao, et al.,

Figure 1

COVERAGE DEPENDENT HREELS STUDY

OF $SiCl_4/Si(100)-(2\times1)$

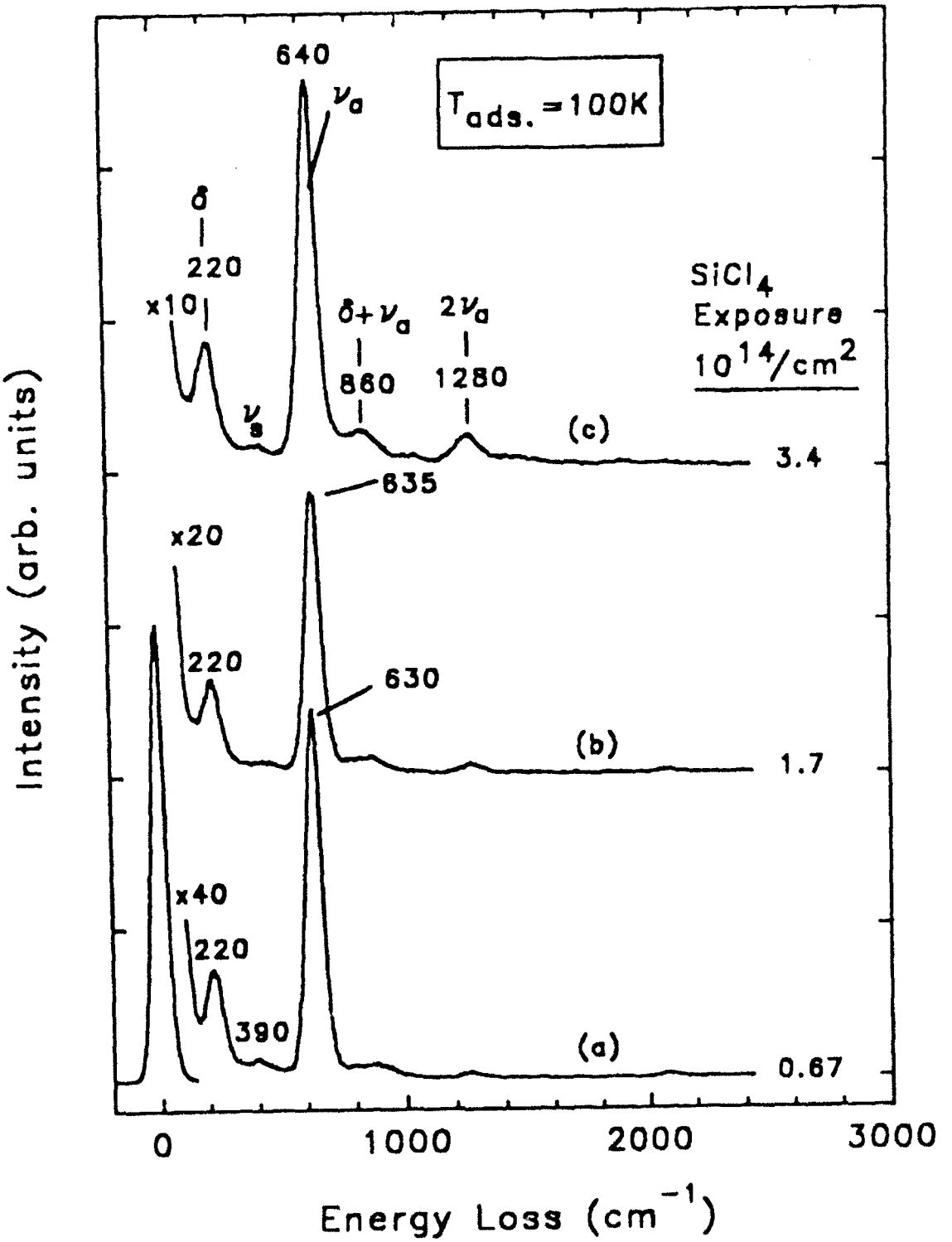

Gao, et al.,

Figure 2

HREELS MEASUREMENTS OF THE THERMAL BEHAVIOR OF $SiCl_4/Si(100)-(2X1)$

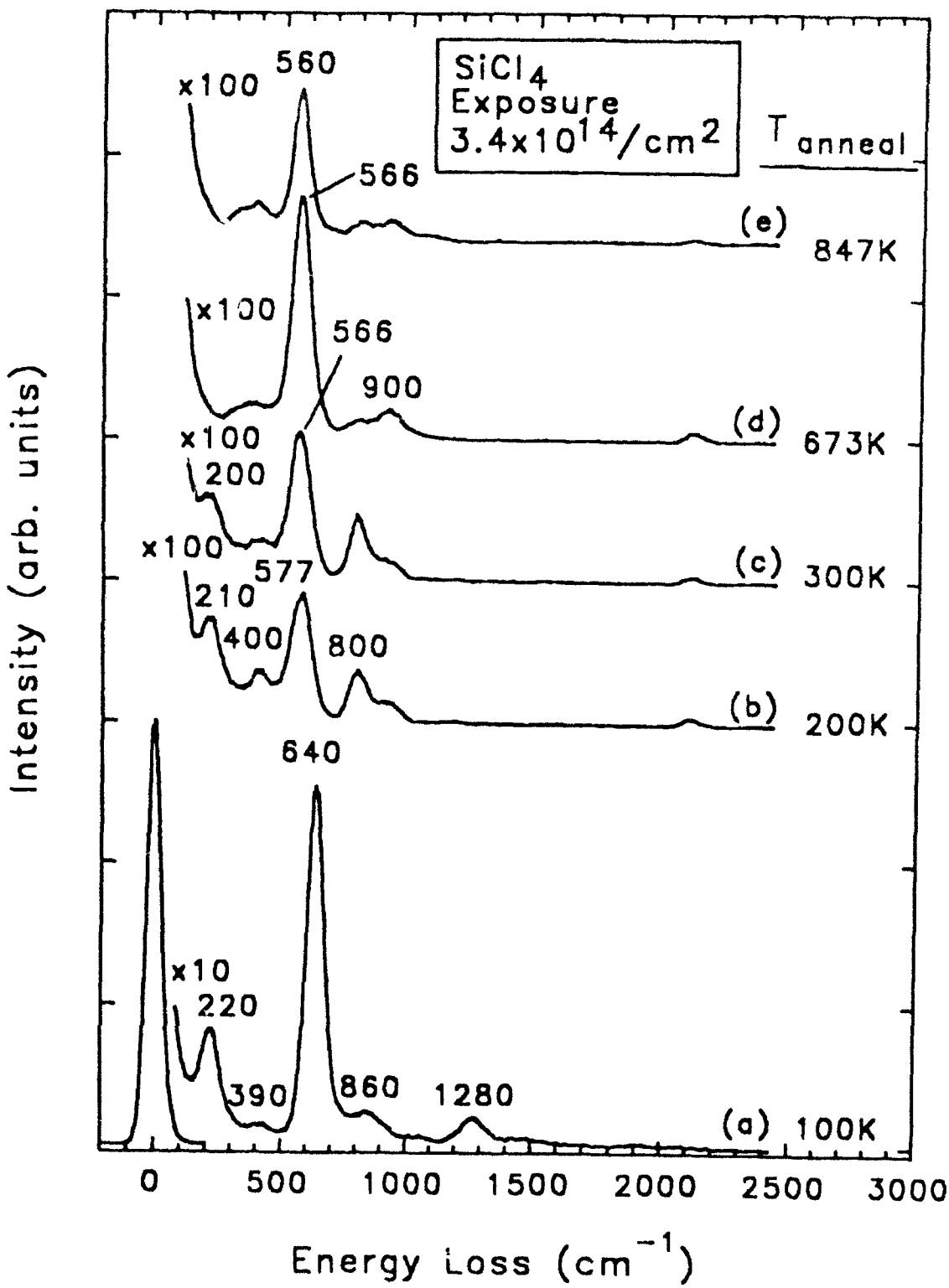

Gao, et al.,

Figure 3

THERMAL DEVELOPMENT OF Cl^+ ESDIAD PATTERN – $SiCl_4/Si(100)-(2\times1)$

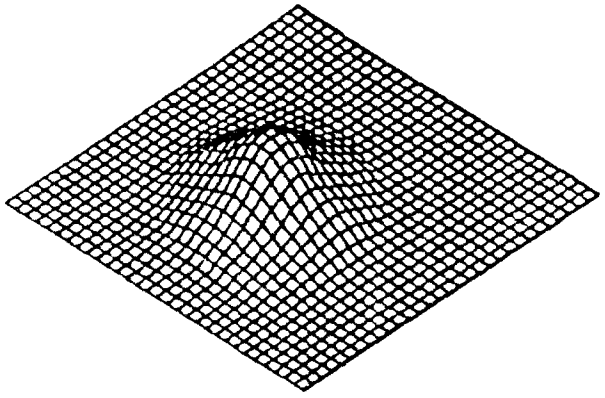

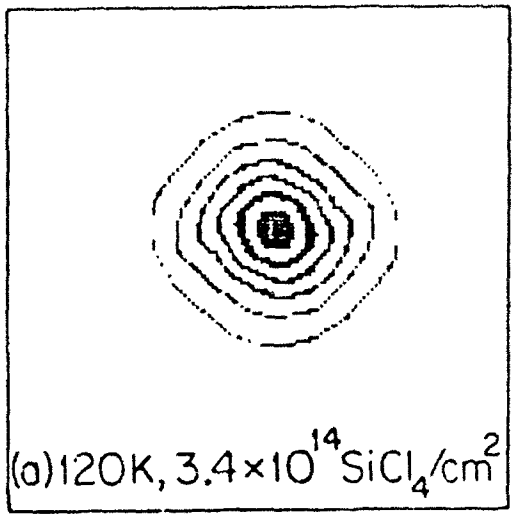

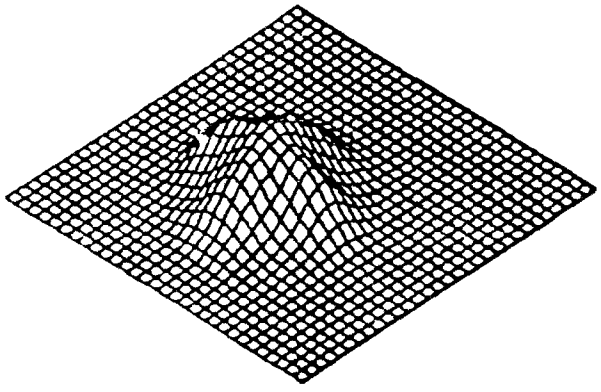

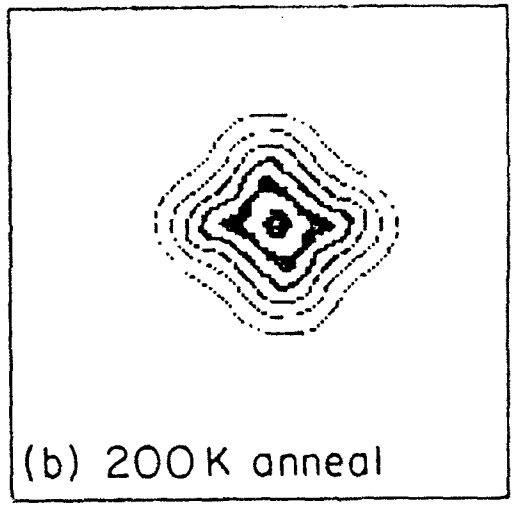

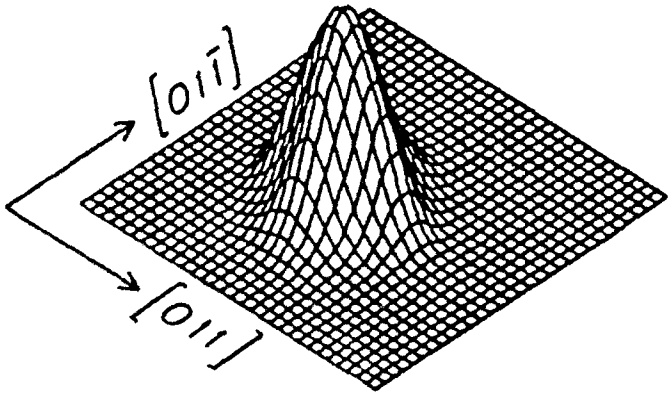

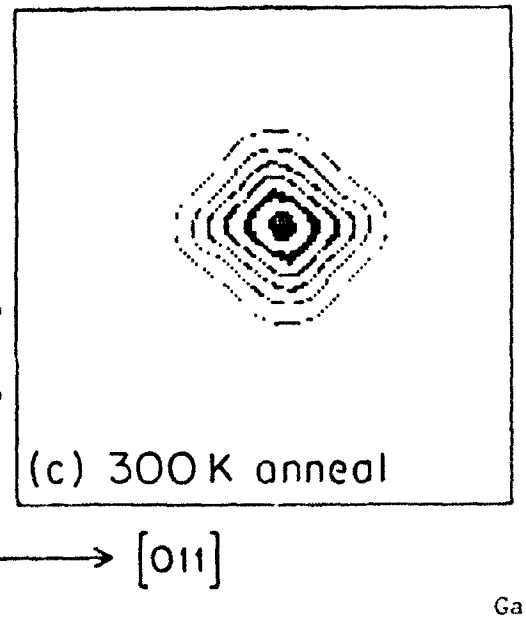

Gao, et al.,

Figure 4

THERMAL DEVELOPMENT OF Cl^+ ESDIAD PATTERN – $SiCl_4/Si(100)-(2\times1)$

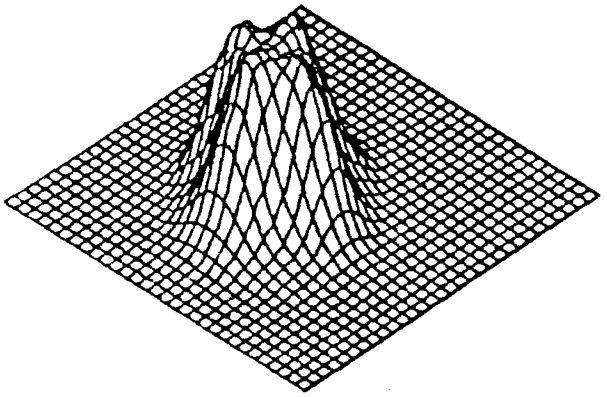

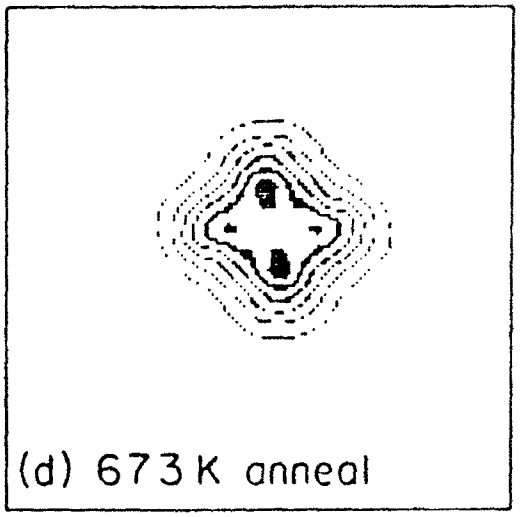

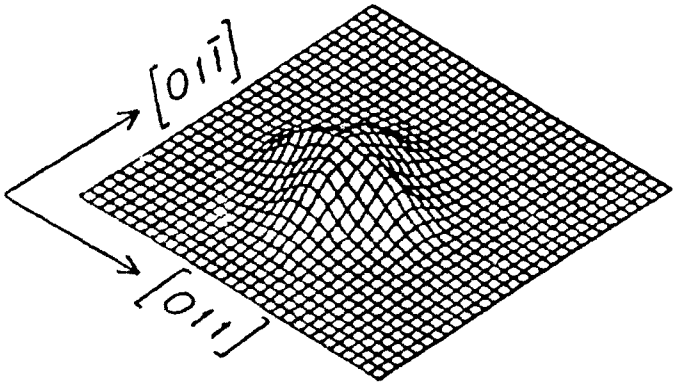

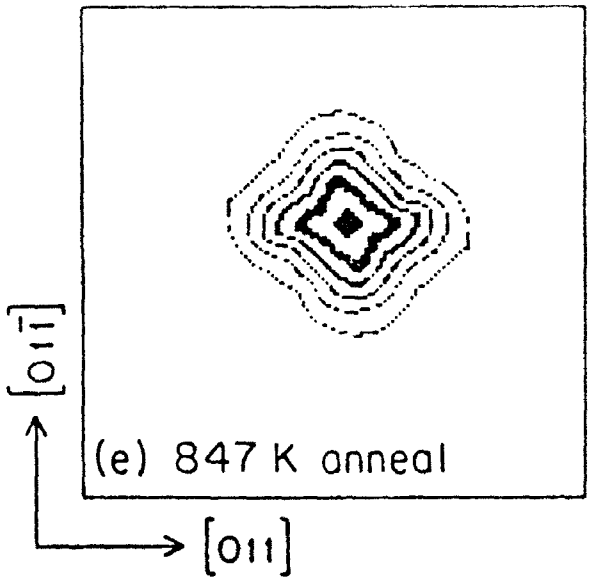

Gao, et al.,

Figure 4
Continued

ALE Contractor Distribution List	# Copies
D.T.I.C. Bldg # 5, Cameron Station Alexandria, VA 22314	12
Dr. Andrew Freedman Aerodyne Research, Inc. 45 Manning Road Billerica, MA 01821 Tel: (508) 663-9500 FAX: (508) 663-4918 e-mail: aerodyn@mitvma.mit.edu	1
Dr. Asif Kahn APA Optics 2950 NE 84th Lane Blaine, MN 55434 Tel: (612) 784-4995 FAX: (612) 784-2038 e-mail: 70702.2032@compuserve.com	1
Dr. Duncan Brown Advanced Technology Materials, Inc 7 Commerce Drive Danbury, CT 06810 Tel: (203) 794-1100 FAX: (203) 792-8040	
Dr. Peter Norris EMCORE Corp. 35 Elizabeth Ave. Somerset, NJ 08873 Tel: (201) 271-9090	1
Prof. Joe Greene Dept. of Materials Science and Engineering University of Illinois 1101 W. Springfield Ave. Urbana, IL 61801 Tel: (217) 333-0747	1
Dr. T. P. Smith IBM T.J. Watson Research Center P. O. Box 218, Route 134 Yorktown Heights, NY 10598 e-mail: trey@ibm.com	1
Prof. Robert F. Davis N.C.S.U. Box 7907	1

Raleigh, NC 27695-7907
Tel: (919) 515-2377/3272
FAX: (919) 515-3419
e-mail: davis@mte.ncsu.edu

Prof. Salah Bedair
Department of Electrical Engineering
N.C.S.U.; Box
Raleigh, NC 27695
Tel: (919) 515-2336
e-mail: jll@@ecegrad.ncsu.edu

1

Max N. Yoder
ONR Code 1114
Arlington, VA 22217
Tel: (703) 696-4218
FAXes (703) 696-2611/3945/5383
e-mail: yoder@charm.isi.edu

1

Dr. A. M. Goodman
ONR, Code 1114
Arlington, VA 22217
Tel: (703) 696-4218
FAXes (703) 696-2611/3945/5383
e-mail: goodman@ocnr-hq.navy.mil

1

Dr. J. Pazik
ONR Code 1113
Arlington, VA 22217
Tel: (703) 696-4410
FAXes (703) 696-2611/3945/5383
e-mail: pazik@ocnr-hq.navy.mil
pazik%estd.decnet@ccf.nrl.navy.mil

1

Prof. J. T. Yates, Jr.
Dept. of Chemistry
Surface Science Ctr.
University of Pittsburgh
Pittsburgh, PA 15260
Tel: (412) 624-8320
FAX: (412) 624-8552
e-mail: yates@vms.cis.pitt.edu

1

Robert J. Markunas, R.A. Rudder
Research Triangle Institute; Box 12194
Research Triangle Park, NC 27709-2194
Tel: (919) 541-6153
FAX: (919) 541-6515
e-mail: rjmk@rti.rti.org

1

Professor Mark P. D'Evelyn
William Marsh Rice University
Dept. of Chemistry
P.O. Box 1892
Houston, TX 77251
Tel: (713) 527-8101, ext. 3468
FAX: (713) 285-5155
e-mail: mpdev@@langmuir.rice.edu

1

Dr. Howard K. Schmidt
Schmidt Instruments, Inc.
2476 Bolsover, Suite 234
Houston, TX 770054
Tel: (713) 529-9040

FAX: (713) 529-1147
e-mail: hksionwk@ricevm1.rice.edu

Prof. A. F. Tasch 1
Dept. of Electrical Engr. & Computer Science
Engineering Science Bldg.
University of Texas at Austin
Austin, TX 78712
Tel:
FAX:
e-mail: tasch@roz.ece.utexas.edu

Prof. Charles Tu 1
Dept of Electrical & Computer Engr.
UCSD
LaJolla, CA 92037
Tel: (619) 534-4687
FAX: (619) 534-2486
e-mail: cwt@celece.ucsd.edu

Prof. John E. Crowell 1
Department of Chemistry
University of California at San Diego
LaJolla, CA 92037
Tel: (619) 534-5441
FAX: (619) 534-0058
email: jcrowell@ucsd.edu

Prof. P. Daniel Dapkus 1
University of Southern California
University Park
Los Angeles, CA 90089-1147
e-mail: dapkus@mizar.usc.edu
Tel: (213) 740-4414
FAX: (213) 740-8684

Unless you are a small business invoking your 2 year proprietory rights clause, you MUST state on the front page of your report: Approved for Public Release; distribution unlimited.